Journal of Engineering Research Innovation and Scientific Development
2(1): 37-53, 2024, https://doi.org/10.61448/jerisd21245
Print ISSN 2971-6594 Online ISSN 2971-6608
www.jerisddelsu.com

Application of Satellite Observation and GIS in Mapping Greenhouse Gases in Part Delta State, Nigeria

E.T. Ogbomida[1], C.N. Emeribe[2*], A.A. Bichi[3], O.A. Ibanga[4]

[1,2]*National Centre for Energy and Environment, Energy Commission of Nigeria, University of Benin*
[3]*Department of Geography, Federal University Gusau, Nigeria*
[4]*Department of Geography and Regional Planning, University of Benin, Benin City, Nigeria*

**Corresponding author: emeribe.c@ncee.org.ng (C.N. Emeribe)*

Article History
Received: 02-01-24
Revised: 02-03-24
Accepted: 24-03-24
Published: 06-04-24

ABSTRACT
The present study aimed to apply satellite observation and Geographic Information System (GIS) to map GHGs in Delta State, Nigeria. Carbon monoxide (CO), nitrous oxide (N_2O), and sulfur dioxide (SO_2) constituted the main GHGs studied. The datasets covering January 2019 to December 2022 were sourced from the archive of Copernicus Atmosphere Monitoring Service Emissions of Atmospheric Compound and Compilation of Ancillary Data. The Google Earth Engine framework, the inverse distance weighting interpolation algorithm in ArcGIS 10.8 software, and Microsoft Excel were deployed in data analyses. In general, the results showed remarkable seasonal oscillation in the mean concentration of CO, with peak values in January and February, while the lowest mean concentration was observed in October. Higher values of NO_2 were observed from November to February and the lowest values in July. July also recorded the highest SO_2 values, with the lowest mean observable atmospheric concentrations in August, in addition to remarkable insignificant values in 2020–2022. Besides, the 12 geospatial models (maps) also depicted the spatio-temporal distribution of CO, NO_2, and SO_2 concentrations from 2019 to 2022 for easy visualization and facilitation of workable policies towards global warming mitigation. The paper recommended the establishment of well-equipped and functional ground-based GHG observatories with early warning systems across the state. This will facilitate real-time GHG monitoring, early warning forecasts, and stimulate scholarship on global warming and climate change.

Keywords: Green House Gases; anthropogenic emissions; Geographic Information Systems; Mapping; Delta State.

1. Introduction

The contribution of greenhouse gases (GHGs) to global warming and climate change, both locally, regionally, and globally, is well documented (Manabe 2019; Mikhaylov *et al*., 2020; Neale *et al*., 2021; Hui *et al*., 2022; Forster *et al.,* 2023). Although GHGs are known to be emitted naturally via permafrost, volcanic activities, wetlands, earthquakes, oceans, and wildfires, anthropogenic activities such as large-scale agriculture, energy exploitation and utilization, industries, automobiles, transportation, cooking, etcetera are considered principal sources of emission, especially since the end of the 20th century (Xi-Liu and Qing-Xian, 2018). Research has shown that while CO_2 seems to dominate climate change and global warming debates, CH_4 and N_2O have also been reported to pose serious threats to the environment (Science Learning Hub, 2018). Global warming and associated climate change have implications for economic development as rising surface temperatures and evapotranspiration affect seasonal rainfall patterns, floods, sea levels, droughts, desertification, etc. The need, therefore, for the collection of an accurate dataset of GHGs with the view to ascertaining their concentration in the lower atmosphere is vital in unraveling the shifts in addition to tracking mitigation efforts over time.

In the last five decades, technological revolution and advancement in space technology have facilitated seamless monitoring, assessment, and mapping of global environmental change indicators, including greenhouse gases (GHGs) worldwide. The increase in the concentration of GHGs in the earth's atmosphere has also led to heightened interest in determining their sources (European Space Agency, 2020). Among the emerging technologies capable of effectively tracking, measuring, assessing, and mapping GHGs is the use of satellite-based remote sensing (RS) and geographic information systems (GIS) (Aganaba-Jeanty and Huggins, 2019). Policymakers across the globe are in dire need of reliable information to understand the dynamics of climate change and hence sustainably address the negative environmental impacts. GIS has been defined as a compendium of computer-based tools used in collecting, analyzing, and mapping spatial data (Garajeh *et al.,* 2023). This function of mapping spatial data comes in handy when putting measures in place to checkmate GHG emissions.

Apart from identifying emission sources, GIS and remote sensing technologies aid in quantifying emission rates, as reported by Thorpe et al., (2022). In Europe and Asia, the application of RS and GIS in mapping greenhouse gases is well documented (Mamatkulova *et al.,* 2022; Dehkordi *et al.,* 2022; Sîrbu et *al*., 2022; Hashim *et al.,* 2023) among others.

In order to support policies on GHG mitigation, Sîrbu *et al., (*2022) used non-proprietary GIS software to estimate the luminosity of solar radiation, and the results in maps were used in planning solar-powered stimulated systems in Timiș County, Romania. Hashim *et al.,* (2023) also used sniffer4D sensors onboard an airborne drone to monitor and measure GHG concentrations, namely NO_2, O_3, CO_2, SO_2, and CH_4, in Pasir Gudang as well as Tanjong Langsat industrialized neighborhood in Malaysia. The finding portrayed a high positive correlation between the remotely sensed GHGs dataset and in-situ data deployed for reliability checks. Carbon dioxide merged as the most prominent GHG, measuring about 625.24 mg/m3, while the level of CH_4 was 249.24 mg/m^3, and the combination of O_3 and NO_2 yielded 249 µg/m^3, even as SO_2 was as high as 115.1 µg/m^3. The overall findings of the Hashim et *al.,* (2023) study showed spatio-temporal disparities and changes in GHG levels across the study, thus aiding appropriate authorities in monitoring commitments towards emission reductions.

A number of studies on the application of GIS in the assessment and mapping of GHGs have also been carried out in several locations in Nigeria. These include, among others, Adedeji *et al*., (2016), who utilized an in-situ GHGs dataset measured by handheld sensor devices to map GHGs emitted by automobiles in Ijebu-Ode, Ogun State, and found that all the GHGs investigated (SO_2, CO, NO_2, along with NO) exceeded allowable established limits. Chukwuma et *al.,* (2018) used the GIS interpolation algorithm to estimate the volume of CH_4 emitted at abattoirs, and Onitsha North as well as Idemili North LGAs emerged as the top emitters of CH_4, which can be leveraged in biogas generation in Anambra State. Salami *et al*., (2019) used a remotely sensed CO_2 dataset and integrated the dataset with urban land-use and land-cover details in compiling CO_2 high-risk zonation maps in Abuja. The findings showed a substantial rise in CO2 emissions over time, with as high as 402.2 ppm in 2016 and a peak level in the AYA roundabout. Similarly, Okpobiri *et al*. (2023) were able to demonstrate the utilitarian worth of GIS in mapping GHGs along

the Gulf of Guinea, Nigeria, using a remotely sensed earth observation dataset. This study found a rising trend of CO_2 levels in the atmosphere at an annual rate of 2.43, with a 63% possibility of the trend reoccurring in the future, with a high value in the dry season.

As laudable and beneficial as RS and GIS use in GHG mapping, the literature reviewed clearly demonstrates the paucity of literature with respect to RS-based satellite observation and GIS applicability in mapping GHGs in Delta State, being an oil-rich state. This calls for research concern, hence, this study aimed to adopt RS-based satellite observation and GIS to map GHGs in the study area.

2. Materials and Methods

2.1 Research Location

The study area is Delta State, one of the oil-rich states in the Niger Delta region of Nigeria. Geographically, Delta State is situated between latitudes 4°55'13.211" and 6027'33.308 north of the Equator and longitudes 4°27'57.288" and 6016'28.085 east of Greenwich. With reference to other states and notable spatial features in the country, Delta State shares its northern boundary with Edo State, while the eastern boundary is shared with Anambra and Rivers States. The southern border is shared with Bayelsa State, while the western border is shared with Ondo State and the Atlantic Ocean, as seen in Figure 1. Delta State has a total of 25 local government areas (LGAs), spanning a landmass of about 17,239.24 km2 (National Population Commission, 2010). Delta State has a characteristically hot-humid climate with temperatures as low as 200 °C and as high as 370 °C, rainfall ranging from 2000mm to 4000mm, relative humidity (70–100%), and typical cloudy sky conditions throughout the year (Peel *et al*., 2007; Mobolade and Pourvahidi, 2020). Most areas experience early morning foggy weather, while solar radiation in the afternoon is painfully glaring with remarkable calm to stumpy wind speed and localized thunder-storm activities. The vegetation is generally luxuriant, with gleysols (G), dystric nitosols (ND), and thionic fluvisols (JT) as the three dominant soil groups, each with unique physical and chemical characteristics.

2.2 Datasets and Sources

Carbon monoxide (CO), nitrous oxide (N_2O), and sulfur dioxide (SO_2) constituted the main GHGs investigated in this study. The datasets covering January 2019 to December 2022 were sourced from the Copernicus Atmosphere Monitoring Service's (CAM) Emissions of Atmospheric Compound and Compilation of Ancillary Data (ECCAD) website. The GHGs dataset consists of an assortment of gridded monthly emission temporal profiles from anthropogenic pollution source categories, namely: energy industry, residential combustion, manufacturing industry, road transport, and agriculture, with guaranteed data quality and consistency (Junker and Liousse, 2008; Höglund-Isaksson, 2012; Klimont *et al.,* 2013; Granier *et al*., 2019).

Figure 1: Delta State Showing Senatorial Districts and LGAs

The rationale for deploying remotely sensed satellite observation in the study was based on cost effectiveness, widespread availability in user-friendly format, easy data processing via the Google Earth Engine (GEE) framework, and smooth spatial and temporal coverage. Remotely sensed satellite observation has also enjoyed widespread applicability in numerous empirical studies relating to air pollution, global warming, and climate change. This can be seen in the works of Anand and Monks (2017) in Hong Kong and Filonchyk et *al*., (2020) in eastern China. Opio *et al*., (2021) and Savenets *et al.,* (2022) also utilized remotely sensed satellite observation in the assessment of GHG concentration in the East African region and Ukrainian territory, respectively.

Other researchers who have also recently explored the utilitarian values of remotely sensed satellite observation in air pollution studies around Konya district in Turkey are Bugdayci *et al*., (2023), while Mejía *et al*., (2023) mapping focused on Guayaquil territory in Ecuador. A more comprehensive detail of the remotely sensed satellite CO, N2O, and SO2 observations, including the metadata, has been provided by Filonchyk *et al*., 2020; Mejía et *al*., 2023).

2.3 Analytical Frameworks

A number of analytical procedures were deployed in the analyses and presentation of the remotely sensed satellite observation. The initial step involved the creation of monthly NetCDF raster layers of all the studies GHGs with the aid of the GEE framework. In this phase, a total of 144 NetCDF raster layers, with 48 each, containing gridded CO, NO_2, and SO_2 data from 2019–2022, were created. In order to map the concentration of GHGs across Delta State, the *extract-values-to-point* algorithm in GEE was deployed in the extraction of CO, NO_2, and SO_2 from the Sentinel-5P layers. The extracted layers, which were in vector formats, were exported in *Comma-Separated Values* (CSV) format, which allowed the GHGs datasets to be saved in table-structured format. It is the exported CO, No_2, and SO_2 layers that were imported into ArcGIS 10.8 software and Microsoft Excel for further analyses.

On the one hand, the study adopted the exported dataset to analyze the seasonal variation of GHGs in Delta State. The determination of the seasonal variation of GHGs simply entailed the summation of daily measurements and observations to arrive at a monthly value and then plotting the monthly figures with the respective months using a combined bar chart in Microsoft Excel. Hink *et al*. (1996) asserted that the most systematic, logical, and coherent approach used in presenting quantitative data is the use of a combined bar chart. The combined bar charts were able to capture and display the concentration of CO, SO_2, and NO_2 in the respective senatorial districts from January 2019 to December 2022.

Conversely, in the ArcGIS 10.8 environment, respective smoothed surfaces were generated for 2019, 2020, 2021, and 2022 using the inverse distance weighting (IDW) interpolation algorithm based on Chukwuma et *al.,* (2018), Salami *et al*., (2019), Ibanga *et al.,* (2022), and Okpobiri *et al.,* (2023). The IDW is a deterministic interpolation framework that uses at least 12 neighboring known points to estimate values for other unsampled locations (Mejía et *al.,* 2023). The newly generated interpolated raster layers of CO, NO_2, and SO_2 in 2019, 2020, 2021, and 2022 were thereafter reclassified into *Very High, High, Moderate, Low, and Very Low* for the purpose of hotspot and cold-spot identification.

3. Results and Discussion

3.1 Seasonal Variation of Greenhouse Gases in Delta State

GHGs, which are also categorized as essential climatic variables (ECVs), vary seasonally across the globe. This motivated us to initiate a probe into the monthly variation of CO, SO_2, and NO_2 from January 2019 to December 2022, and the results are presented in Figures 2–5. Carbon (ii) oxide showed remarkable seasonal oscillation in the mean concentration, with February emerging as the month in 2019 with peak values of 0.067 ppm in the Delta South and Delta Central SDs, while the Delta North SD recorded a mean value of 0.071 ppm, as seen in Figure 2. On the other hand, October also emerged as the month with the lowest mean

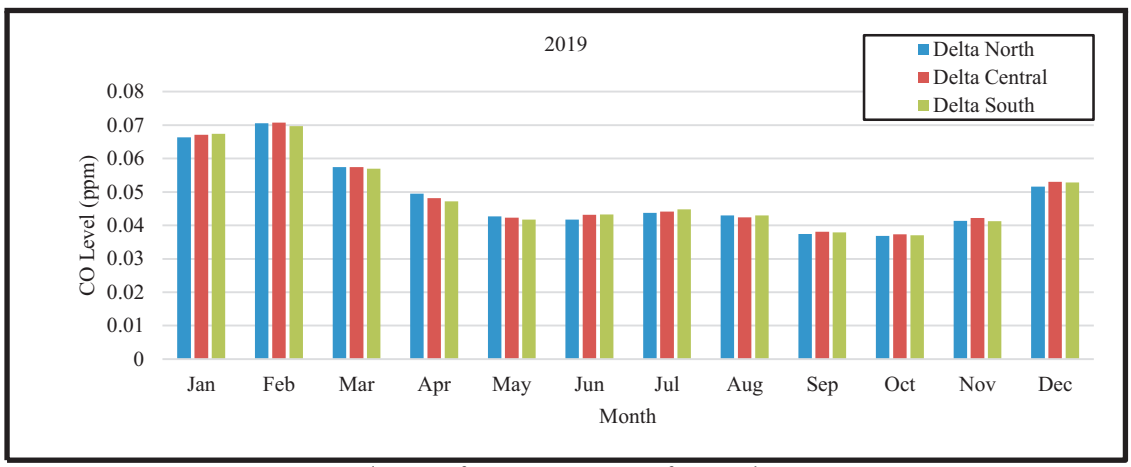

Figure 2: Seasonal Pattern of Mean Concentration of CO in Delta State in 2019

A similar pattern of mean concentration of CO was observed in 2020, 2021, and 2022. In 2020, for instance (Figure 3), Delta South SD had 0.077 ppm, Delta Central SD (0.078 ppm), and Delta North SD (0.075 ppm). The lowest mean value of 0.037 ppm was observed in Delta South and Delta Central SDs, along with 0.036 ppm observed in Delta North SD. In 2021, January emerged in Delta South and Delta Central SDs as the month with the highest mean concentration of 0.066 ppm, whereas it was February in Delta North (0.064 ppm), as evidenced in Figure 4. In 2022 (Figure 5), Delta South SD had 0.066 ppm, Delta Central SD (0.068 ppm), and Delta North SD (0.067 ppm). The lowest mean value of 0.036 ppm was observed across the three SDs in October.

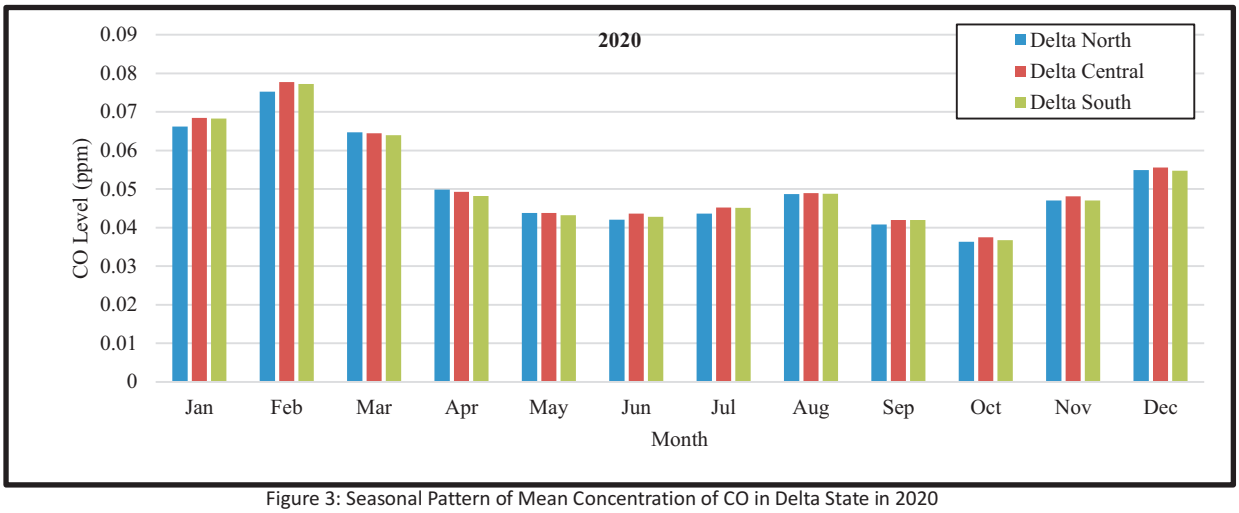

Figure 3: Seasonal Pattern of Mean Concentration of CO in Delta State in 2020

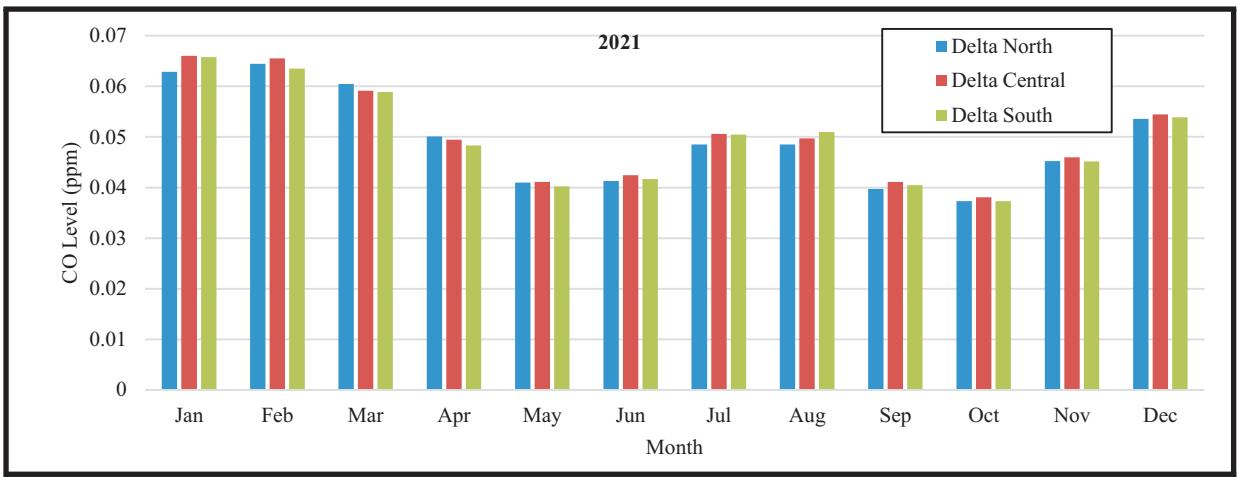

Figure 4: Seasonal Pattern of Mean Concentration of CO in Delta State in 2021

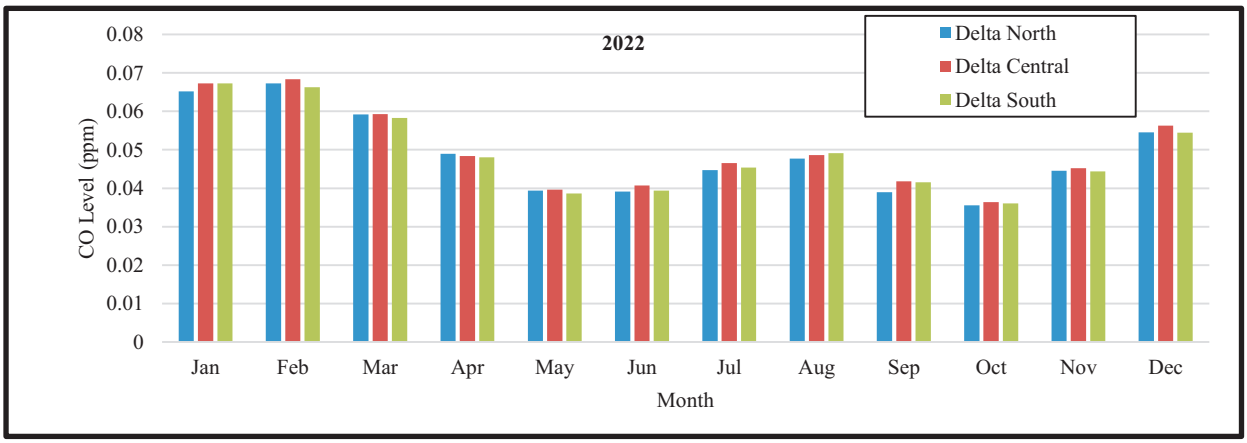

Figure 5: Seasonal Pattern of Mean Concentration of CO in Delta State in 2022

In 2019, January surfaced as the month with the peak mean atmospheric concentration of NO_2 in Delta South SD (6.2×10^{-4} ppm) and Delta Central SD (7.11×10^{-4} ppm), even as it was February (7.0×10^{-4} ppm) in Delta North SD, as witnessed in Figure 6. August also emerged as the month with the lowest mean atmospheric concentration of NO_2, with 4.3×10^{-4} ppm in Delta South SD, 4.42×10^{-4} ppm in Delta Central SD, and 4.6×10^{-4} ppm in Delta North SD.

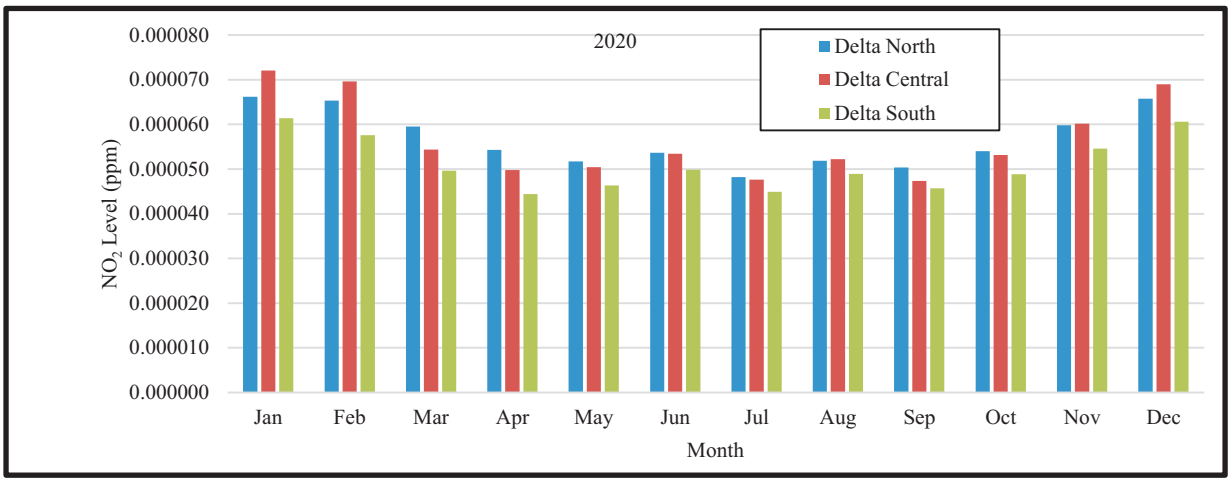

Figure 6: Seasonal Pattern of Mean Concentration of NO_2 in Delta State in 2019

January again surfaced as the month in 2020, with a peak mean atmospheric concentration of NO_2 in Delta South SD (6.1 x 10^{-4} ppm) and Delta Central SD (7.2 x 10^{-4} ppm) just as it was 6.6 x 10^{-4} ppm in Delta North SD, as witnessed in Figure 7. Conversely, July also emerged as the month with the lowest mean atmospheric concentration of NO_2, with 4.5 x 10^{-4} ppm in Delta South SD, 4.76 x 10^{-4} ppm in Delta Central SD, and 4.8 x 10^{-4} ppm in Delta North SD.

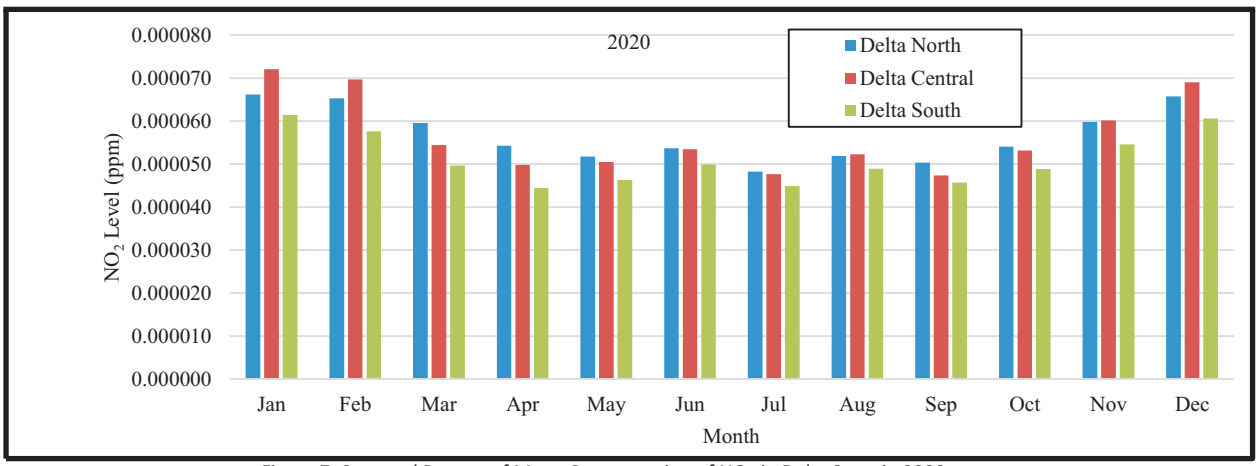

Figure 7: Seasonal Pattern of Mean Concentration of NO_2 in Delta State in 2020

In 2021, the month with the highest mean atmospheric concentration of NO_2 moved to December in all the SDs, with Delta South SD recording 6.9 x 10^{-4} ppm, Delta Central SD (7.82 x 10^{-4} ppm), and 7.6 x 10^{-4} ppm in Delta North SD, as witnessed in Figure 8. August still remained the month with the lowest mean atmospheric concentration of NO_2, with 4.9 x 10^{-4} ppm in Delta South SD, 5.14 x 10^{-4} ppm in Delta Central SD, and 5.3 x 10^{-4} ppm in Delta North SD. In 2022, the month with the highest mean atmospheric concentration of NO_2 shifted back to January in all the SDs, with Delta South SD recording 7.1 x 10^{-4} ppm, Delta Central SD (8.18 x 10^{-4} ppm), and 7.4 x 10^{-4} ppm in Delta North SD, as witnessed in Figure 9. Also, the month with the lowest mean atmospheric concentration of NO_2 returned to July with 4.6 x 10^{-4} ppm in Delta South SD, 5.03 x 10^{-4} ppm in Delta Central SD, and 5.0 x 10^{-4} ppm in Delta North SD.

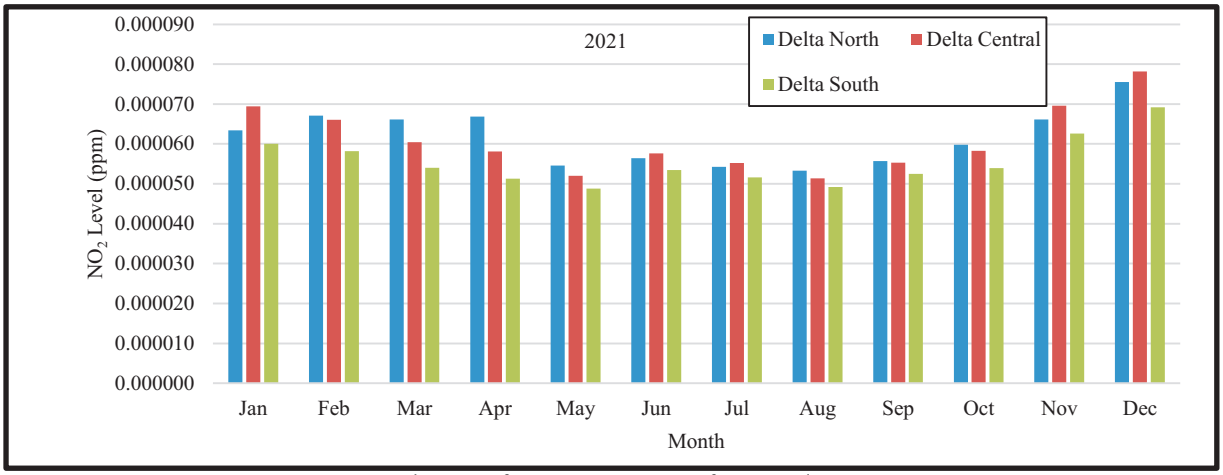

Figure 8: Seasonal Pattern of Mean Concentration of NO_2 in Delta State in 2021

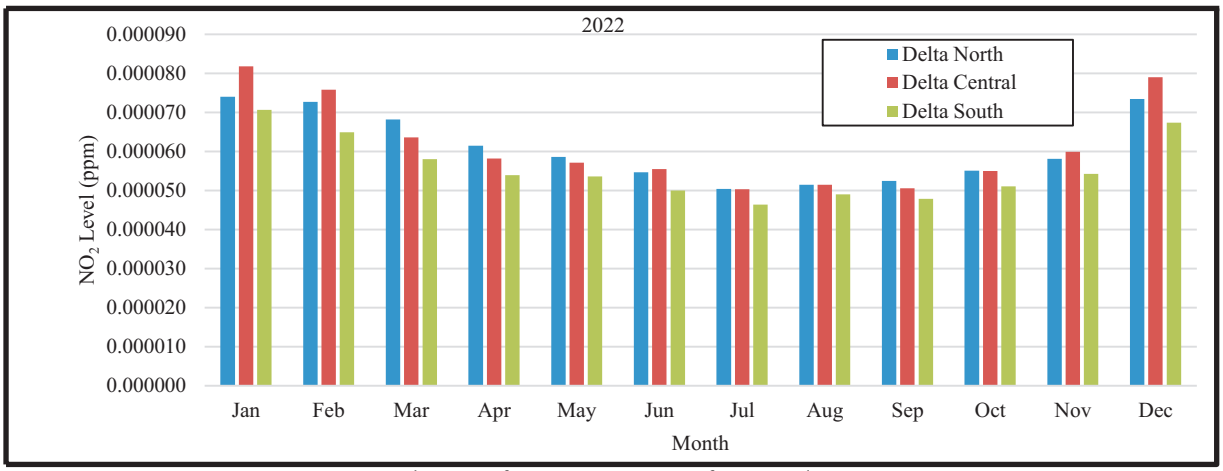

Figure 9: Seasonal Pattern of Mean Concentration of NO_2 in Delta State in 2022

With respect to the seasonal pattern of mean concentration of SO_2 in 2019, July recorded the highest values of 5.7×10^{-4} ppm in Delta South SD, 6.6×10^{-4} ppm in Delta Central SD, and 5.9×10^{-4} ppm in Delta North SD (Figure 10). August also emerged as the month with the lowest mean observable SO_2 level in the atmosphere, with 1.6×10^{-5} ppm in Delta South SD, 5.5×10^{-5} ppm in Delta Central SD, and 1.0×10^{-5} ppm in Delta North SD. In 2020, substantial volumes of SO_2 (0.0331 ppm in Delta South SD, 0.183 ppm in Delta Central SD, and 0.130 ppm in Delta North SD) were noticed in September (Figure 11). In 2021 (Figure 12), the month with the highest values of 0.00871pp (Delta South SD), 0.0147ppm (Delta Central SD), and 0.0131ppm (Delta North SD) even as it drifted back to September 2022 (Figure 13), with Delta South SD recording 2.8×10^{-4}ppm, Delta Central SD (7.79 x 10-2ppm), and Delta North SD (5.86×10^{-2}ppm). Other months recorded traced and/or negligible concentrations of SO_2 across the study period and location.

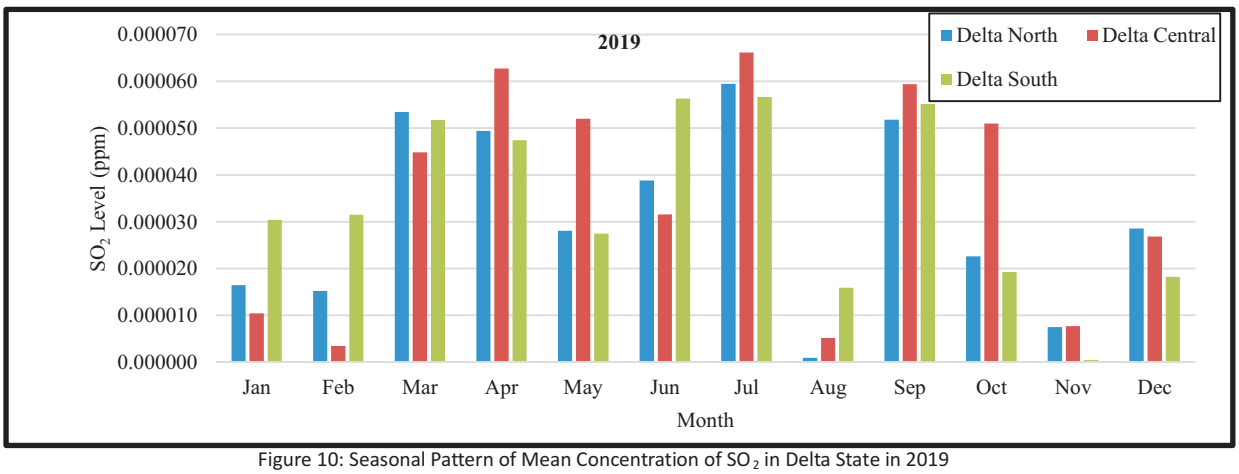

Figure 10: Seasonal Pattern of Mean Concentration of SO_2 in Delta State in 2019

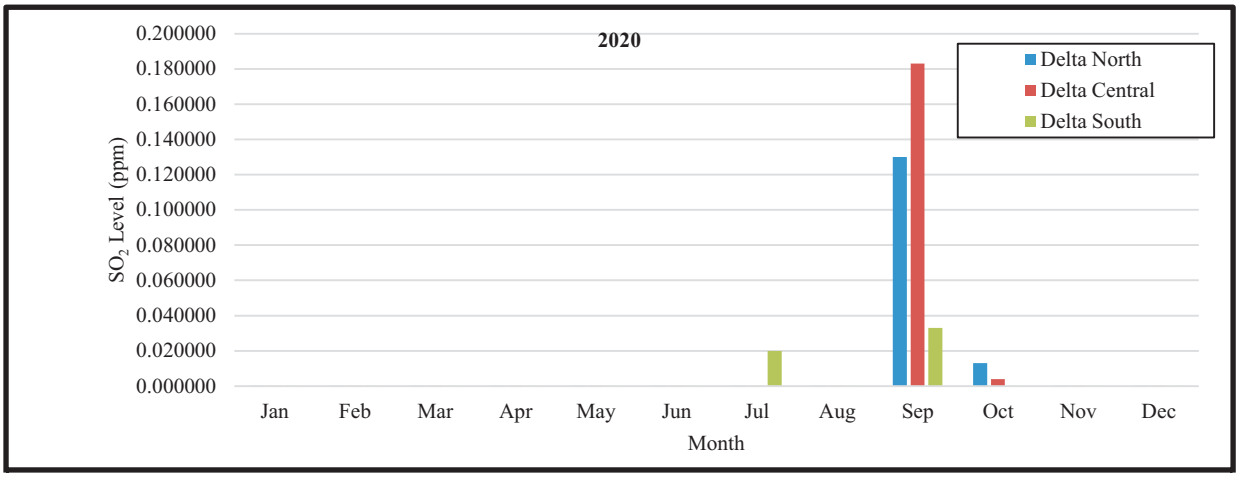

Figure 11: Seasonal Pattern of Mean Concentration of SO_2 in Delta State in 2020

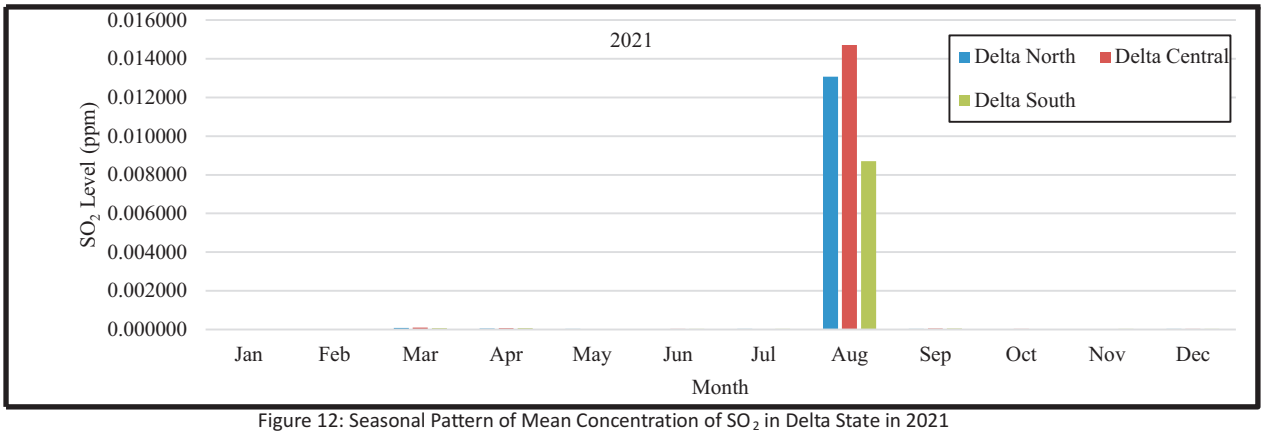

Figure 12: Seasonal Pattern of Mean Concentration of SO_2 in Delta State in 2021

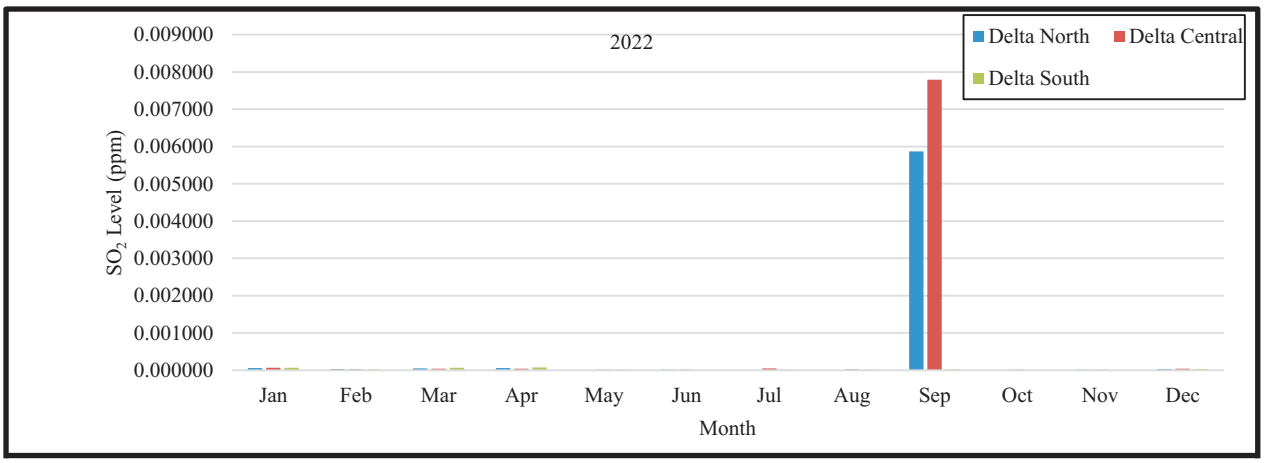

Figure 13: Seasonal Pattern of Mean Concentration of SO_2 in Delta State in 2022

In general, it could be noticed that all the GHGs studied exhibited almost the same pattern of variations monthly in the study period across the state. Elevated atmospheric concentrations were observed during the peak dry season (December to February) and reduced values during the rainy season (May to September). These findings are in agreement with the results of previous studies undertaken by, among others, particularly in tropical regions. For instance, Sheel *et al*. (2014) reported that atmospheric as well as dissimilarity across seasons are profound indications of the extended influence of the intertropical zone of discontinuity (the doldrum) and bush/waste fire in addition to the wet and dry states created by the El Niño-La Niña shift. Shehu *et al.* (2019) also attributed the seasonal variation of GHGs to season and the influence of insolation from the sun, a function of the percentage of cloud cover in the sky. The authors opined that rain is known to inhibit the uplift of air pollutants from the ground surface and mixing with air, while this is more prominent in drier atmospheres.

Besides, a decrease of 1 Kwh/m^2/day incident energy from the sun also reduced up to 8.42% of CO, 1.7 Kwh/m^2/day approximately 30% of SO2, and 2.5 Kwh/m^2/day about 3% of particulate matter with a diameter less than 2.5 ($PM_{2.5}$) in the FCT, Abuja (Shehu et *al.,* 2019).

The nature and/or type of activity carried out in a particular land is another determinant of variation in GHGs in any given region, as reported by Obiefuna et *al.,* (2021). They found that the highest mean value of 3.2 ppm CO was recorded in commercial land use, with a peak concentration of 3.6 ppm in the dry season and 2.7 ppm in the rainy season in the Calabar metropolitan area. Transport land uses also emerged as top emission sources for NO_2 and SO2, with the peak concentration of NO_2 in the dry season being 2.9 ppm and the wet season reducing to 1.1 ppm. The highest level of 2.9 ppm was recorded against SO_2in the dry season and 2.04 ppm during the rainy season (Obiefuna et *al*., 2021).

Busa *et al*., (2022) linked the seasonal disparity of CO in the lower atmosphere around tropical Indian urban areas to poor and/or reduced denitrifying activities of soil microbes, a rise in micro-discharge of CO, as well as the prevailing planetary wind systems. The abundance and eutrophication activities of phytoplankton in anthropogenic-influenced marine ecosystems have also been found to boost the release of GHGs into the aquatic environment and surrounding atmosphere. Nguyen et *al*., (2022) reported that from 2019 to 2020, Saigon River Estuary, Vietnam, recorded a CO_2 value of 3174 ± 1725 g/liter, which approximately exceeded the average worldwide level by 13 to 18 times.

Eutrophication activities in the study location and period also emitted about 5.9 ± 16.8 µgC-CH4/liter, which was beyond the average worldwide level by 52 to 332 times. Also, N_2O_3 is 37 times greater than the average worldwide level based on enrichment of 3.0 ± 4.8 gN-N_2O/liter in terms of concentration (Nguyen et *al.,* 2022). A study of air pollutants in nine major cities in Nigeria, including Lagos, Illorin, Abuja, Oweri, Enugu, Port Harcourt, Sokoto, Kano, and Maiduguri, between 2005 and 2018, also by David-Okoro et *al*., (2023), also uncovered disparities in GHGs among seasons. Peak atmospheric concentrations of CO (4.801 ppm), NO_2 (3.502 ppm), and SO2 (5.446 ppm) were reported in January and December, with decreased values in wet seasons.

3.2 Geospatial Mapping of Greenhouse Gases Concentration in Delta State

The distribution of phenomena in space, especially global and local environmental change indicators, cannot be more deciphered for an informed decision without visual perusal of such phenomena. Thus, venturing into geospatial mapping of a socio-ecological issue like GHG concentration was another leading stimulus for this study. Our ambitious intent was to facilitate easy visualization of GHG concentration in Delta State in order to boost the evolution of workable policies, prioritizing existing ones, monitoring, and evaluation of efforts towards global warming and climate change mitigation and adaptation. This resulted in the compilation of 12 geospatial models (maps) to depict the spatiotemporal distribution of CO (Figures 14–17), NO_2 (Figures 18–21), and SO_2 (Figures 22–24) concentrations from 2019 to 2022 in Delta State. At the beginning of the study year (Figure 4.35), the central to southern parts, with a subtle spread to the northeastern flank of the state, recorded *very high* CO concentrations ranging from 0.0491 to 0.0504 mol/m^2. *Moderate* CO concentrations (0.0484-0.0487 mol/m^2) can still be seen dotting the

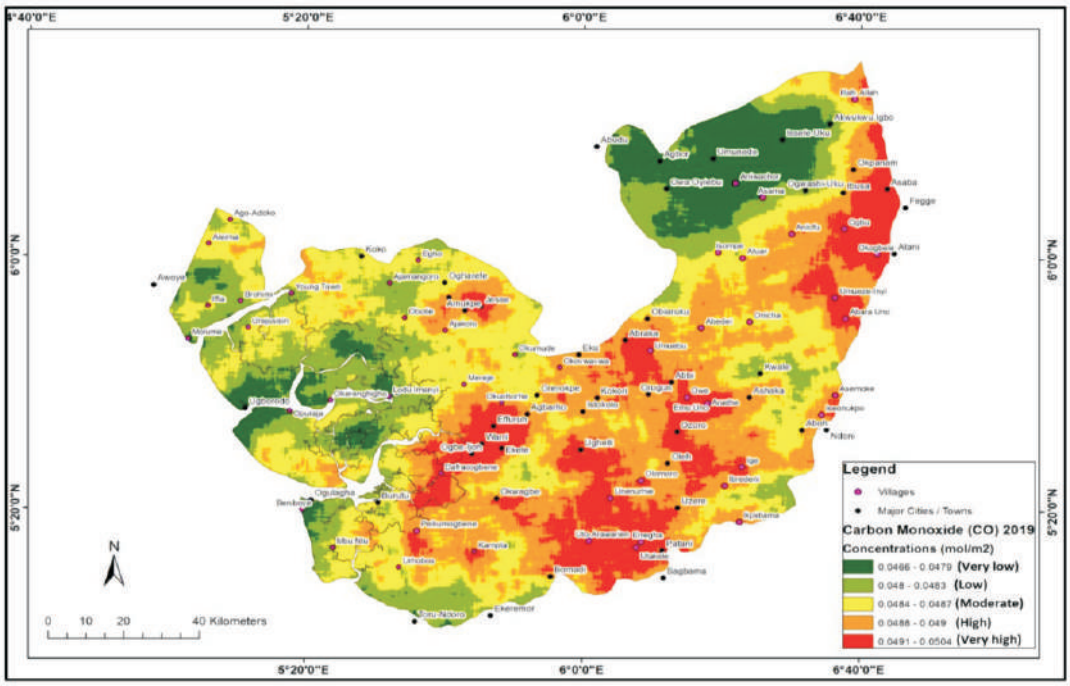

Figure 14: Spatial Distribution of CO Concentration in Delta State in 2019

Among the settlements with *a very high* concentration of CO in 2019 are: Jesse, Effurun, Warri, Ekate, Dafracogbene, Okwagbe, Kampta, Ughelli, Olomoro, Unenurhie, Uto-Arawarien, Erregha, Patani, Utakele, Abraka, Umuebu, Abbi, Owe, Emu Uno, Aradhe, Ozoro, Ogbu, Okogbele, Umueze-Inyi, Abara Uno, Illah, and Asaba. Some of the settlements with *moderate* CO concentrations in 2019 are Aleima, Iffia, Urejusisin, Koko, Egho, Ogbarafe, Obotie, Burutu, Urhobos, Mereje, Onicha, Isompe, and Atuar, among others. In contrast, Ugboroda, Opuraja, Okerenghigho, and Lodu Imenyi settlements in the west, Agbor, Owa Oyiebu, Umuneda, Aniwachor, Issele Uku, and Akwukwu Igbo in the north, among others, had *very low concentrations* of CO.

In 2020, *very high* hotspots of CO concentration with a range of 0.0522–0.0534 mol/m^2 clustered around the central part and northeastern edge of the state, as seen in Figure 15. Key settlements under these hotspots include Eku, Okovwavwa, Okuohorhe, Orerokpe, Agbarho, Kokori, Isiokolo, Effurun, Warri, Ekete, Ughelli, Bomadi, Okwagbe, Olomoro, Unenurhie, Uzere, Abedei, Abbi, Orogun, Owe, Emu Uno, Aradhe, Ashaka, and Ozoro. *Moderate* CO concentrations in the range of 0.051-0.0515 mol/m2 were huddled around the west-central and eastern sides of the state, with the most affected settlements being Koko, Egho, Ajamangooro, Atuar, Aniofu, Okogbele, Asemoke, Iseonukpo, and Aboh.

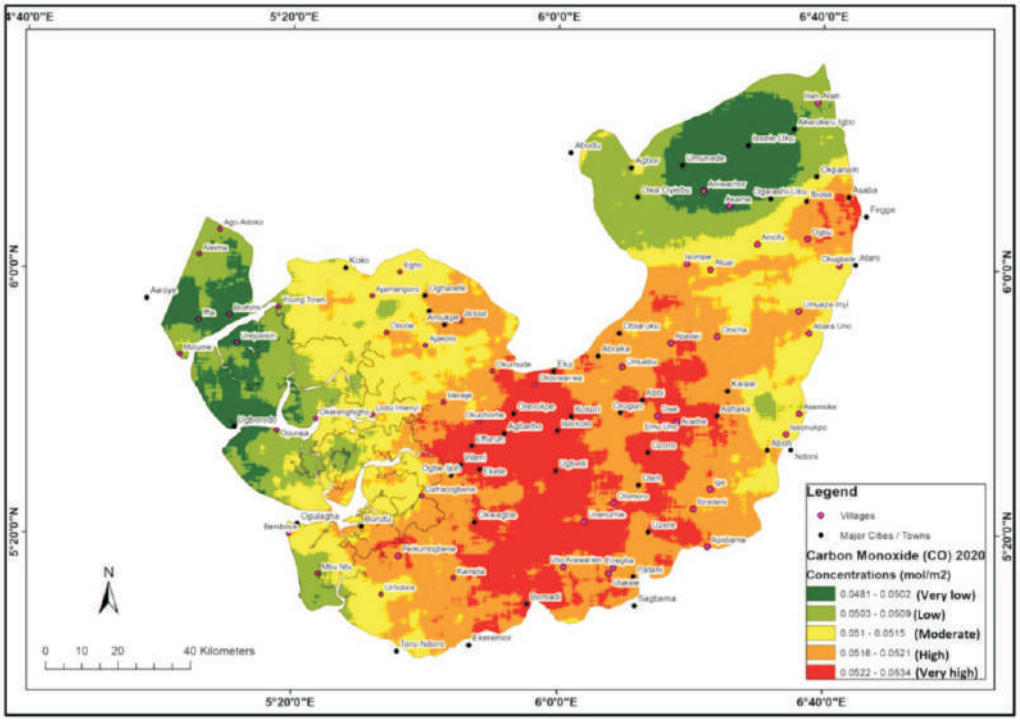

Figure 15: Spatial Distribution of CO Concentration in Delta State in 2020

The western and northern flanks were characterized by *very low* CO concentrations (0.048–1.0502 mol/m^2), with Iffia, Brohimi, Urejusiisin, Ugborodo, Umunede, Issele-Uku, Aniwachor, and Asama as major settlements around them. A similar distributional pattern of CO concentration was noticed in 2021 (Figure 16), with settlements having *very low* CO concentration (0.04696–0.04866 mol/m^2) being Ago-Adoko, Iffia, Brohimi, Umunede, Issele-Uku, Aniwachor, and Owa Oyiebu. Settlements falling under *moderate CO* concentration (0.04928–0.04981 mol/m^2) include Koko, Okerenkoko, Burutu, Mbu Ntu, Ige, Owe, Emu Uno, Aradhe, Ogwashi-Uku, and Illah Town.

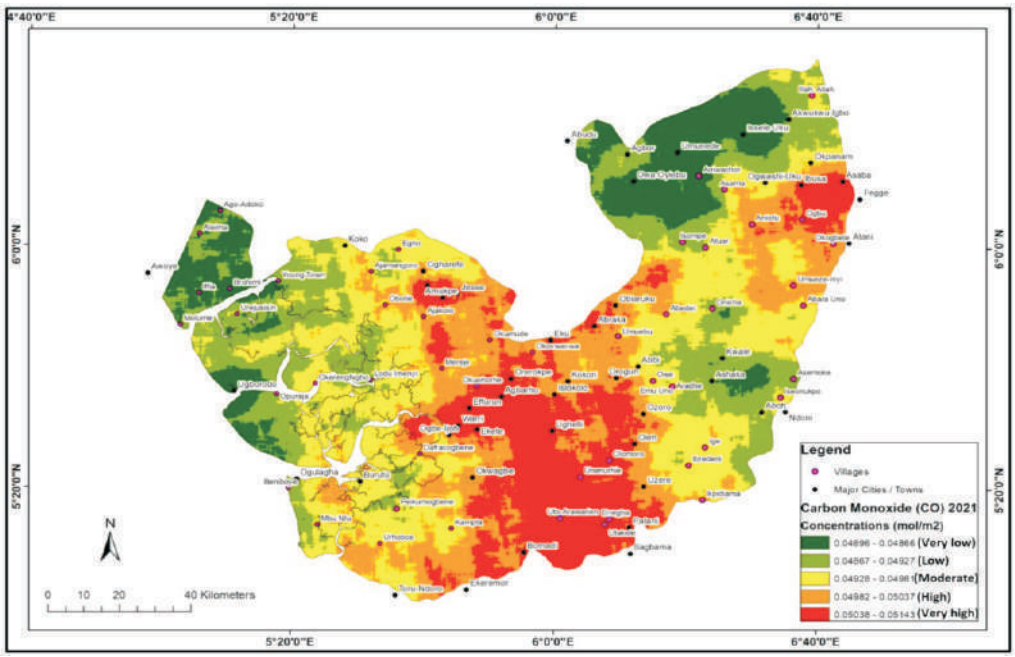

Figure 16: Spatial Distribution of CO Concentration in Delta State in 2021

Major settlements with *very high* CO concentrations (0.05038–0.05143 mol/m^2) include Amukpe, Sapele, Jesse, Eku, Abraka, Okovwavwa, Okuohorhe, Orerokpe, Effurun, Agbarho, Isiokolo, Effurun, Warri, Ekete, Ughelli,Orogun, Oleh, Olomoro, Unenurhie, Uto-Arawarien, Erregha, Patani, Utekele, and Bomadi. In 2022, *very high* CO hotspots (0.05018–0.05108 mol/m^2) gathered around the central part and eastern flank of the state, as evidenced in Figure 4.38. Notable settlements under *very high* CO hotspots include: Okovwavwa, Okuohorhe, Orerokpe, Effurun, Agbarho, Isiokolo, Effurun, Warri, Ekete, Ughelli, Olomoro, Uto-Arawarien, Erregha, Patani, Utekele, and Asaba. *Very low*-CO cold spots include Molume and Ugborodo in the west and Issele Uku and Akwukwu Igbo in the north.

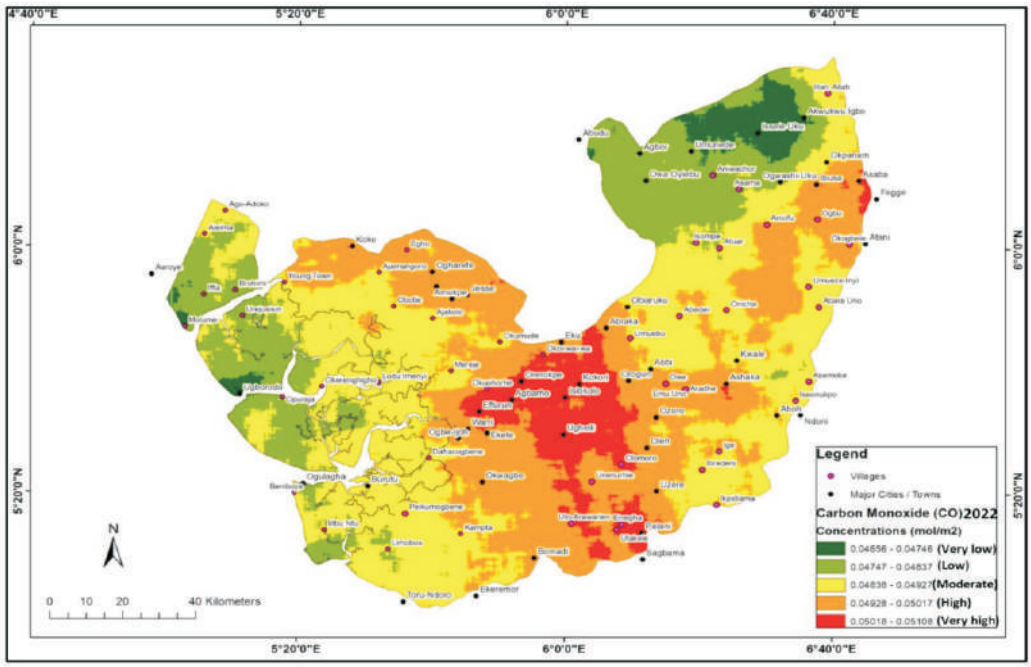

Figure 17: Spatial Distribution of CO Concentration in Delta State in 202 2

Interestingly, nitrogen dioxide (NO_2) concentration followed a peculiar distribution pattern with somewhat yearly similarities across the state. Very high NO_2 hotspots of 5.829–6.722 x 10^{-5} mol/m^2 in 2019 (Figure 18) and 6.091–7.285 x 10^{-5} mol/m^2 in 2020 (Figure 19) were observed around the Warri industrial hub and Asaba administrative and commercial nerve center in the state. Indistinguishable Very high NO_2 hotspots with concentration ranges of 6.781–8.188 x 10^{-5} mol/m^2 were also noticed in 2021 (Figure 20) and 6.698–8.11 x 10^{-5} mol/m^2 in 2022 (Figure 21) around the same Warri industrial hub and Asaba administrative and commercial nerve center in the state.

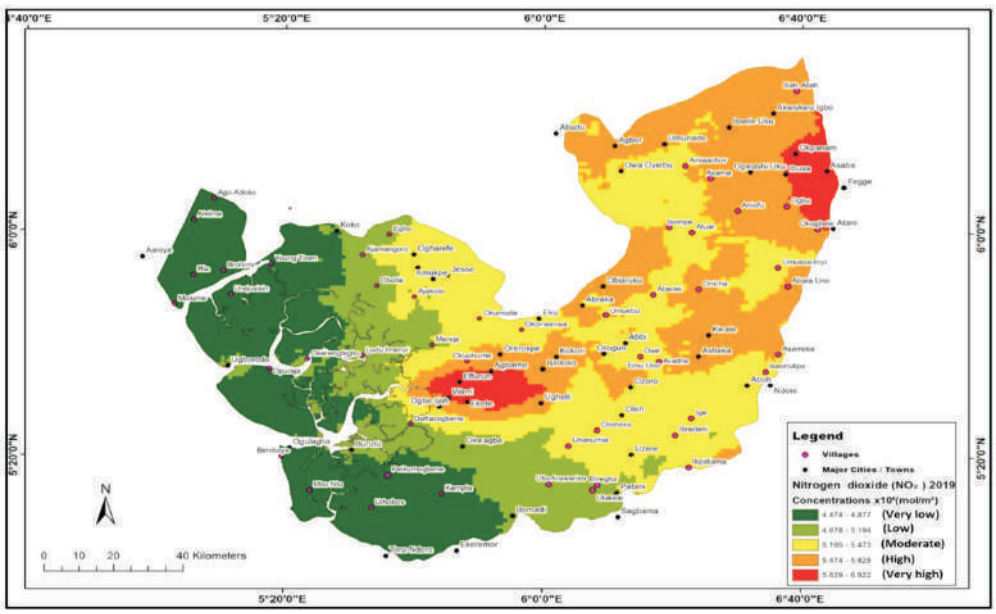

Figure 18: Spatial Distribution of NO_2 Concentration in Delta State in 2019

In contrast, the littoral western flank was characterized by *very low* NO_2 cold spots with a concentration range of 4.965–5.479 x $10^{-5\ mol}$/m^2 in 2019 and 4.54–4.971 x 10^{-5} mol/m^2 in 2020. Analogous *A very lows* patial pattern of NO_2 ranging from 5.012–5.472 x 10^{-5} mol/m^2 in 2021 and 4.965–5.479 x 10^{-5} mol/m^2 in 2022 was spotted in the littoral western flank. Notable settlements found in this *very low* NO_2 *concentration* zone include: Ago-Adoko, Iffia, Brohimi, Young Town, Molume, Urejusisin, Opuraja, Okerenkoko, Lou Imenyi, Burutu, Ogulagha, Beniboye, Mbu Ntu, Peikumogbene, Urhobos, Kampta, and Bomadi.

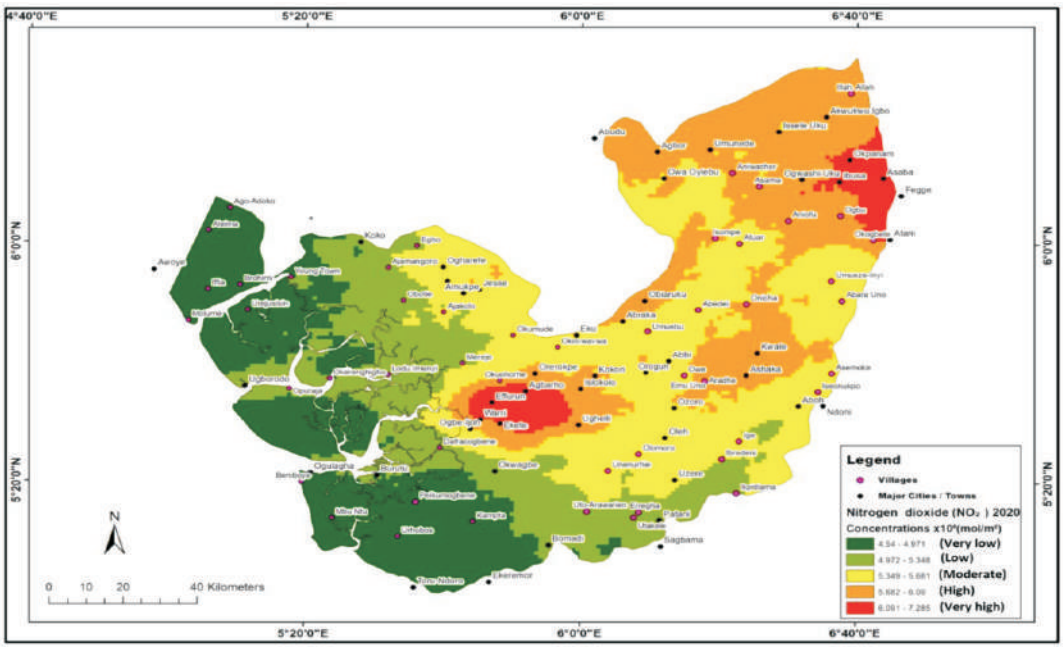

Figure 19: Spatial Distribution of NO_2 Concentration in Delta State in 2020

Also, moderate NO_2 concentration was almost homogeneous across the study period, with a 2019 value ranging from 5.195–5.473 x 10^{-5} mol/m^2 and 5.349–5.681 x 10^{-5} mol/m^2 in 2020. An almost identical pattern of moderate NO_2 concentration with a range of 5.871–6.27 x 10^{-5} mol/m^2 in 2021 and 5.85–6.13 x 10^{-5} mol/m^2 in 2022 was observed in the state. Notable settlements locating within this moderate NO_2 concentration zone from 2019 to 2022 include Ogharefe, Amukpe, Jesse, Ajakolo, Okumude, Eku, Okovwavwa, Oleh, Olomoro, Ige, Ibredeni, Unenurhie, Uzere, Isompe, Atuar, Aboh, and Iseonukpo, among others.

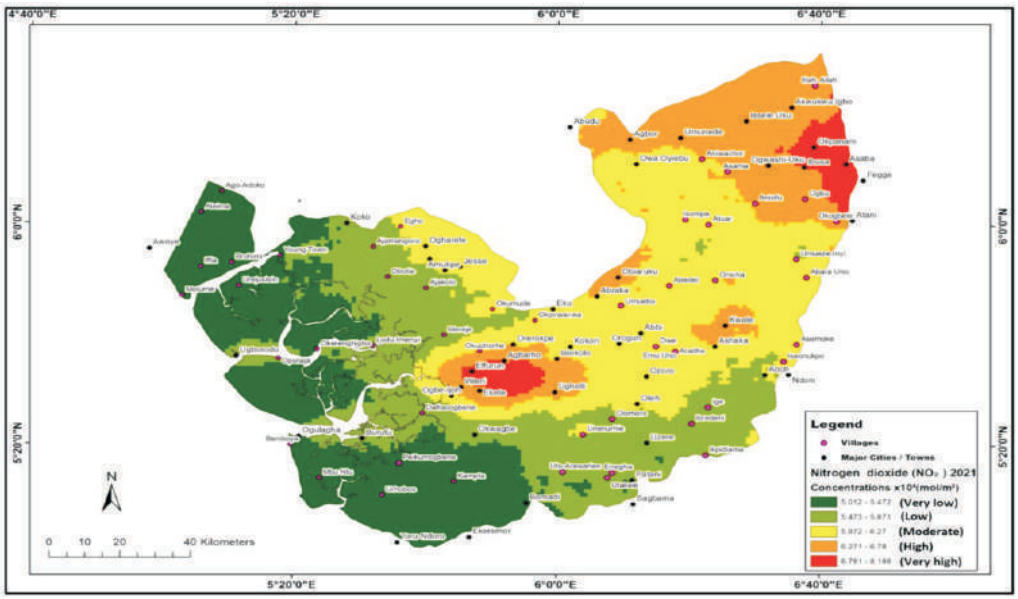

Figure 20: Spatial Distribution of NO_2 Concentration in Delta State in 2021

Besides, imperceptible spatial patterns could also be discerned across the study period regarding locations with *low* and *high* NO_2 concentrations in Delta State. *Low* NO_2 concentration ranged from 4.878 to 5.194 x 10^{-5} mol/m^2. *while high* NO_2 concentration ranged from 5.474 to 5.828 x 10^{-5} mol/m^2 in 2019. In 2020, low NO_2 concentration ranged from 4.972 to 5.348 x 10^{-5} mol/m^2, while *high* NO_2 concentration ranged from 5.682 to 6.09 x 10^{-5} mol/m^2, whereas in 2021, *Low* NO_2 concentration ranged from 5.473 to 5.8718 x 10^{-5} mol/m^2 and *high* NO_2 (6.72 to 6.78 x 10^{-5} mol/m^2). In addition, *low* NO_2 concentrations in 2022 ranged from 5.48 to 5.85 x 10^{-5} mol/m^2, *while* high NO_2 concentrations ranged from 6.184 to 6.697 x 10^{-5} mol/m^2. Settlements conspicuously located within the l*ow* NO_2 concentration zone from 2019 to 2022 include Koko, Ajamangoro, Obotie, Defracogbene, Okwagbe, Uto-Arawarien, Erregha, Bomadi, Utakele, and Patani. Similarly, settlements that are clearly situated within the *high* NO_2 concentration zone from 2019 to 2022 include Okuohorhe, Ororekpe, Isokolo, Obiaruku, Abraka, Kwale, Ashaka, Ogbu, Okogbele, Agbor, Umunede, Ogwashi-Uku, Ogbu, Okogbele, Illah, and Akwukwu Igbo.

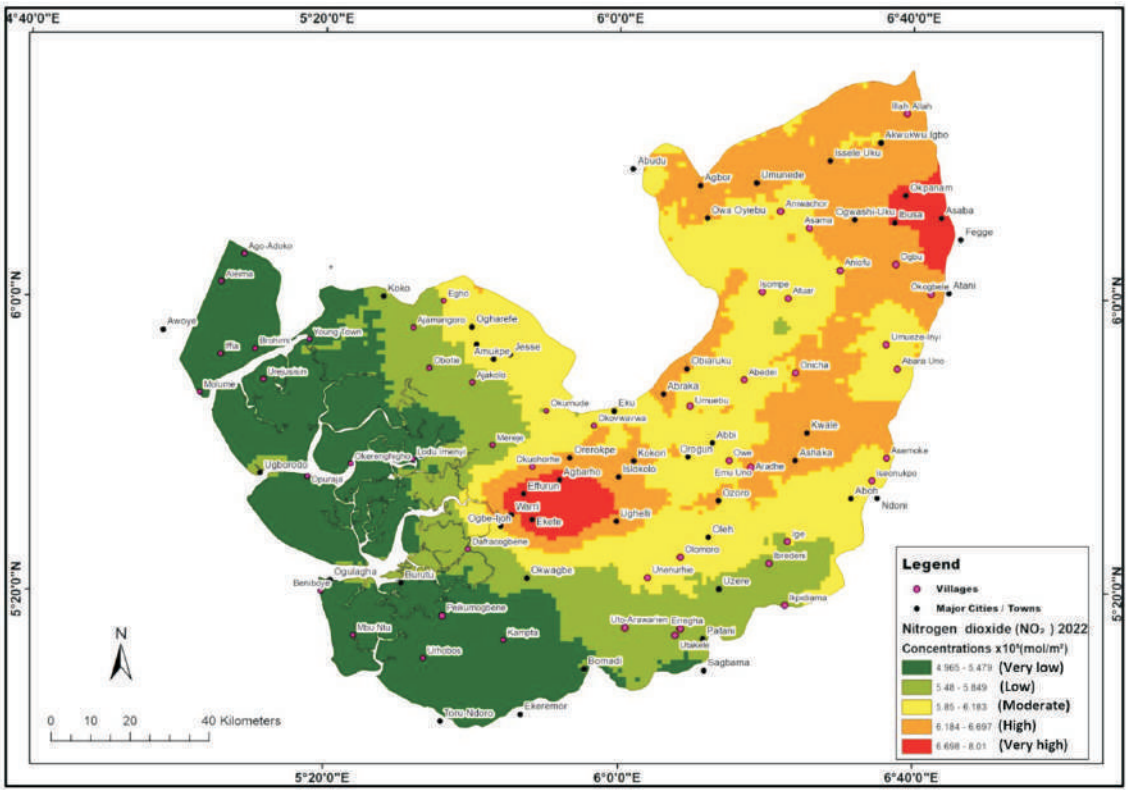

Figure 21: Spatial Distribution of NO_2 Concentration in Delta State in 2022

Another GHG in whose spatial distribution we were interested was So_2, and the spatial models as seen in Figures 22–25 showed that a greater part of Delta State is inundated with an almost insignificant concentration. In 2019, the areas we classified as *high* SO_2 hotspots had a value ranging from 0.000026 to 0.0000537 mol/m^2 (Figures 22), while in 2020, it was 0.000033 to 0.00011 mol/m^2 (Figures 23). Similarly, in 2021, *the* high SO2 hotspot value ranged from 0.000047 to 0.000197 mol/m^2 (Figures 24), even though in 2022, it was 0.00005884 to 0.0001175 mol/m^2 (Figures 25). However, *high* SO_2 hotspots were more prominent across the landscape in 2022 when compared to other years, thus signifying an increase in emissions over time.

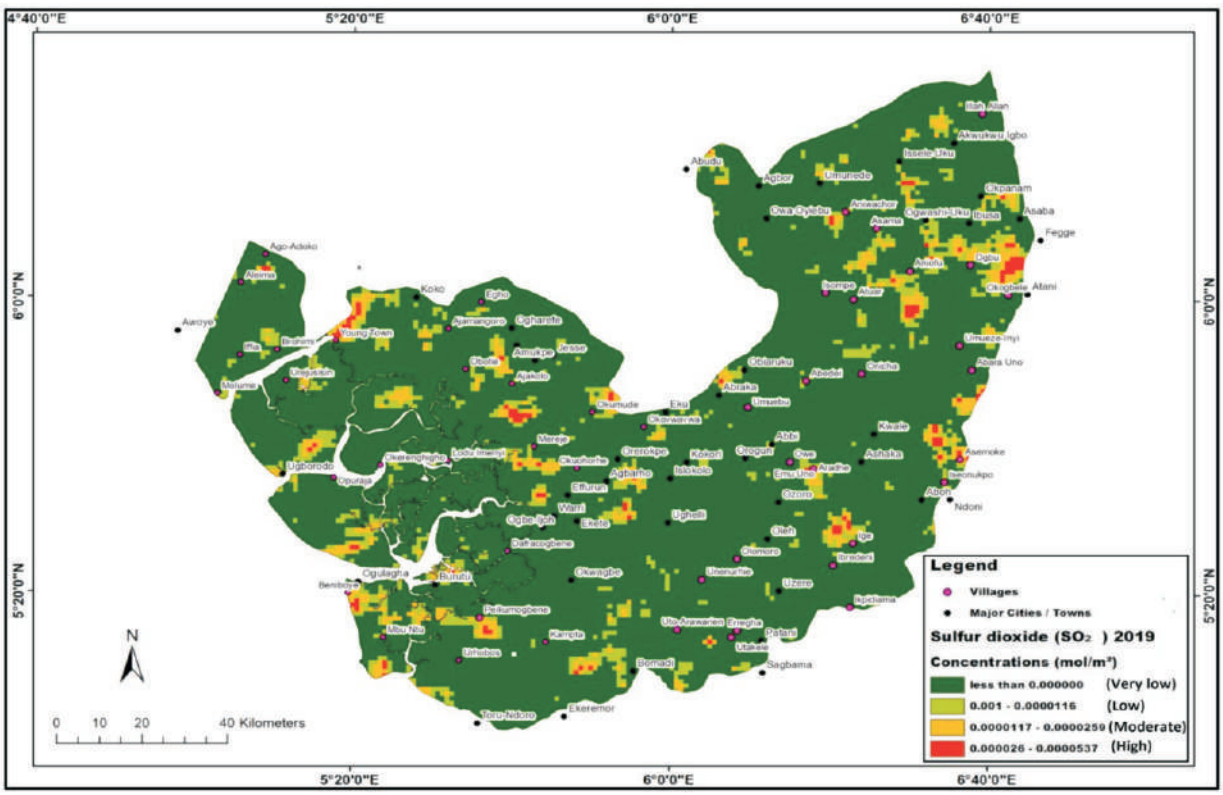

Figure 22: Spatial Distribution of SO_2 Concentration in Delta State in 2019

It was also observed that in 2020, settlements like Aleimalffia, Brohimi, Young Town, Ajakolo, Umuebu, Obiaruku, Ige, Asemoke, Isompe, Atua, and Agbor were located within the zone of *the high* NO_2 hotspot. In 2021, Aleima, Beniboye, Warri, and Atuar were found within the *high* NO_2 hotspot, whereas in 2022, it was Iffia and Egho. Some of the settlements conspicuously found within the *Moderate* NO_2 hotspot (0.000000116–0.00005883 mol/m^2) in 2022 also include Aleima, Brohimi, Molume, Urejusisin, Ugborodo, Opuraja, Obotie, Beniboye, and Urhobos in the western part of the state. Also, Eku, Okovwavwa, Orerokpe, Effurun, Warri, Ogbe-Ijoh, Ughelli, Abbi, Owe, Emu Uno, Aradhe, Ozoro, Uzere, Erregha, Utakele, and Patani, located in the central and south parts of the state, are found within the *moderate* NO_2 hotspots.

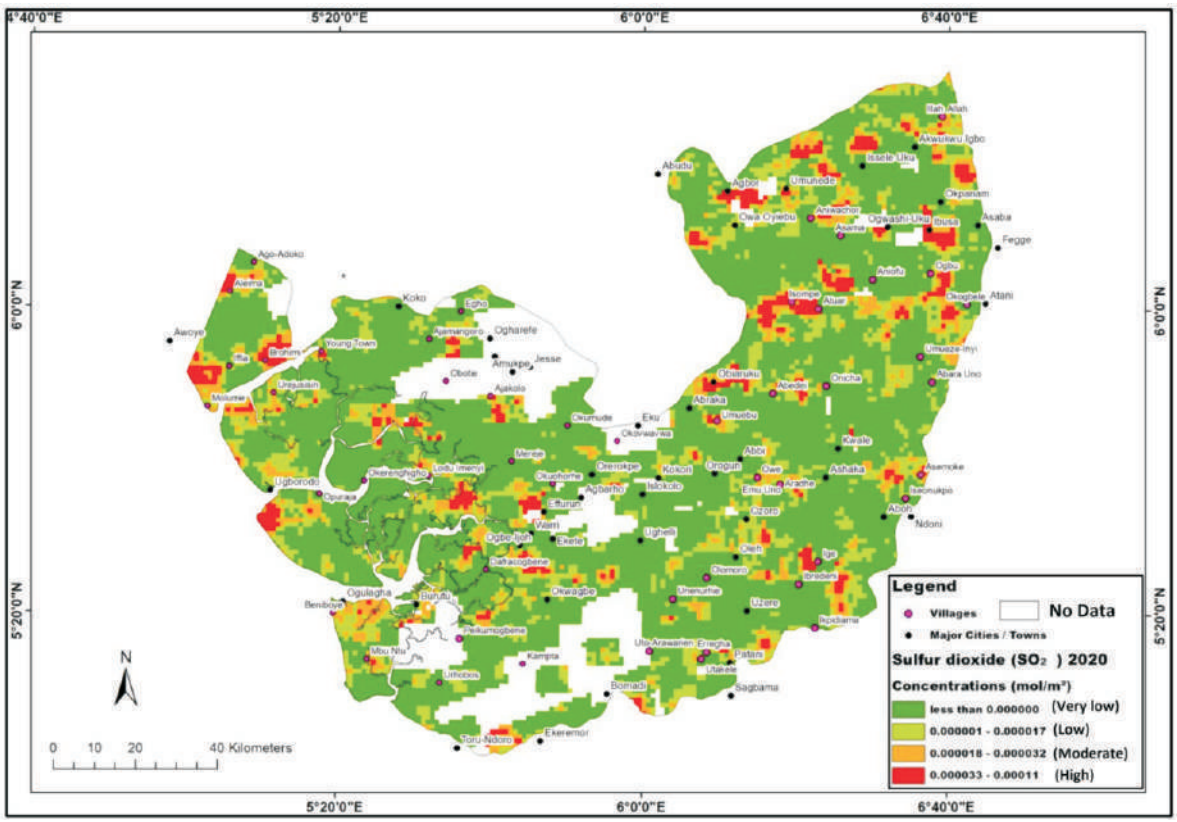

Figure 23: Spatial Distribution of SO_2 Concentration in Delta State in 2020

In the eastern and northern flanks, Asemoke, Iseonukpo, Aboh, Abara Uno, Isompe, Atuar, Aniofu, Ogbu, Okogbele, Agbor, Owa Oyiebu, Aniofu, Ogbu, Okogbele, Okpanam, Ogwashi-Uku, Ibusa, Akwukwu Igbo, and Illah, among others, were also found within the *moderate* NO_2 hotspots. In general, it should be noted that the principal source of the investigated GHGs is anthropogenic, and chief among them is gas flaring, as experienced in many parts of Delta State, as reported by Okoh (2013) and the Delta State Ministry of Economic Planning (2022), among others. Other anthropogenic sources of CO, NO_2, and SO_2 are the energy utilization of fossilized and/or carbonaceous fuels by automobiles, industries, commercial enterprises, household cooking, forest fires, etcetera (Egbe, 2013; Ugboma, 2023; Egwunatumet et *al*., 2022).

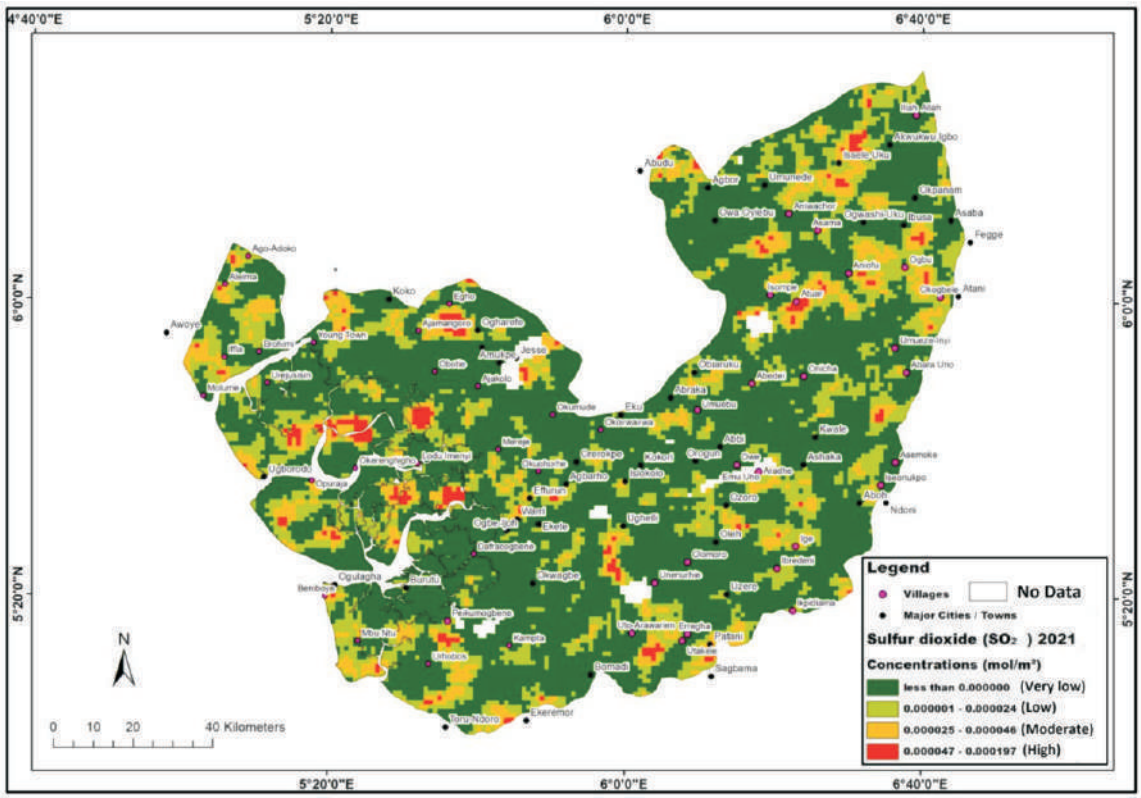

Figure 24: Spatial Distribution of SO_2 Concentration in Delta State in 2021

Moreover, despite the existence of *very high* and *high* hotspots of various GHG annual concentrations, they were comparatively lower than the World Health Organization (WHO, 2021) allowable standards for ambient air quality. This finding, however, corroborates a study around educational land use in an urbanized environment, which indicated that the average NO_2 value of 29.4 µg/m^3 and the median value of 21.1 µg/m^3, although with accompanied health implications, were relatively lower than WHO allowable limits of 40 µg/m^3 yearly exposure (Salonenet et *al.,* 2019). Agbozu and Oghama (2022) also reported analogous lower than established standards of NO_2 level (0.00148 mol/m^3) and SO_2 level (0.00148 0.0036 mol/m3) in educational land use near a coal quarry site in the South African town of Emalahleni.

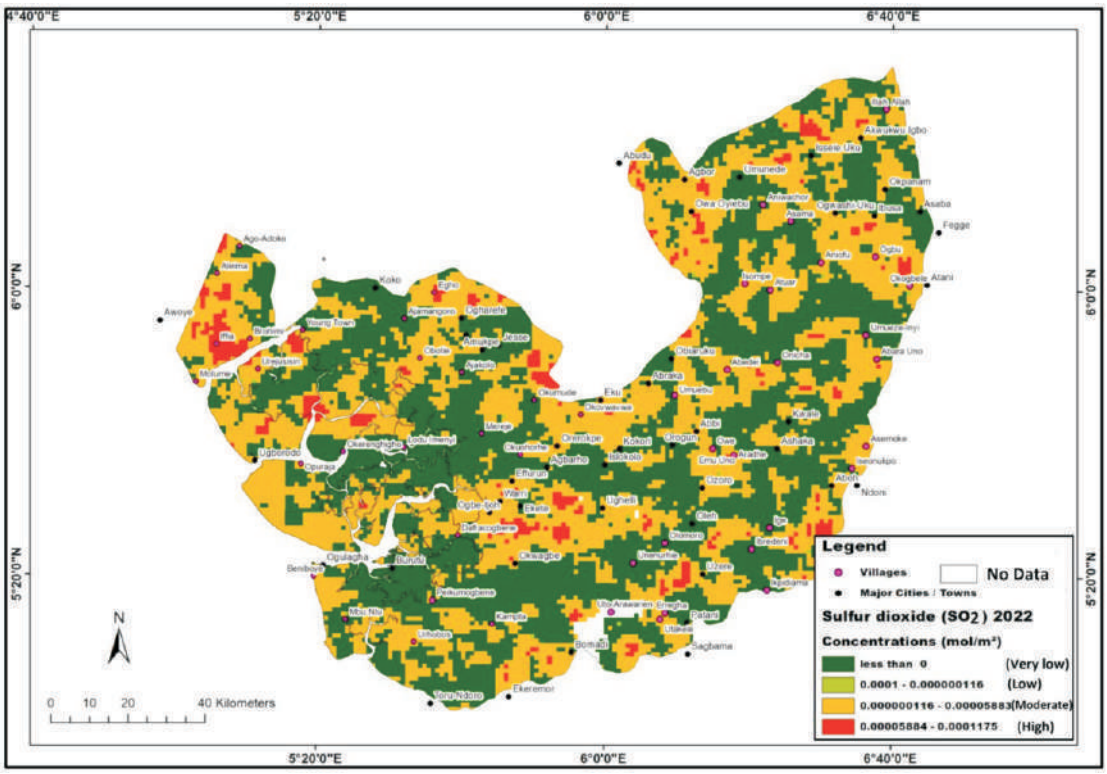

Figure 25: Spatial Distribution of SO Concentration in Delta State in 2022

In contrast, when compared with the results of previous studies conducted by Haşim et *al*., (2023), Adedeji *et al.,* (2016), Agbozu and Oghama (2022), and Erawan *et al*., (2021), CO, NO_2, and SO_2 concentrations were relatively subservient. Adedeji *et al*., (2016) reported higher than WHO limits for CO, which ranged from 4.8–137 ppm, NO_2 (67–302 ppb), and SO_2 (38–245 ppb) in the metropolitan area of Ijebu-Ode, Ogun State. Erawan et *al.,* (2021) reported 0.00854767 g/ms of CO between 0600-0900 hours (UTC) and 0.007938 g/ms between 1500-1800 hours (UTC) in the street of Daan Mogot in the town of Tangerang, Indonesia. Hashim et *al.,* (2023) study also showed CO, NO_2, and SO_2 values exceeding WHO limits with CO (0.41–16.41 mg/m^3), NO_2 (4.72–377.98 g/m3), and SO_2 (13.13–115.10 g/m^3) in metropolitan areas of Pasir Gudang and Tanjung, Malaysia.

4. Conclusion

The study showed clearly temporal and spatial disparities of CO, SO_2, and NO_2 from January 2019 to December 2022 in Delta State, Nigeria. In general, CO showed remarkable seasonal oscillation in the mean concentration, with peak values recorded in January and February, while October was the month with the lowest mean concentration. Regarding NO_2, higher values were observed from November to February, whereas the lowest mean atmospheric concentration was recorded in July. With respect to SO_2, July recorded the highest values, while the lowest mean observable atmospheric concentrations were in August, with remarkable insignificant values during the COVID-19 and post-COVID-19 years. Also, the central to southern parts, with a subtle spread to the northeastern flank of the state, recorded *very high atmospheric* concentrations of CO. Interestingly peculiar spatial patterns with somewhat yearly similarities across the state were also noticed in NO_2, *with very high* hotspots observed around the Warri industrial and Asaba administrative and commercial hubs in the state. Besides, greater parts of Delta State were inundated with an almost insignificant (*very low*) concentration of SO_2. Generally, despite the existence of *very high* and *high* hotspots of various GHG annual concentrations, they were comparatively lower than the World Health Organization's (2021) allowable standards for ambient air quality.

This study undoubtedly underscored the utilitarian functionality of deploying remotely sensed satellite observation and GIS to map GHG concentrations in a typical data-sparse region. The geospatial models, apart from facilitating easy visualization of GHG concentration across the Delta, are capable of aiding stakeholders and policymakers in the evolution of workable policies, prioritizing existing ones, monitoring, and evaluation of efforts towards global warming and climate change mitigation and adaptation. There is therefore a need for the establishment of well-equipped and functional ground-based GHG observatories with early warning systems across the state. This will facilitate real-time GHG monitoring, early warning forecasts, and stimulate scholarship on global warming and climate change.

References

Adedeji, O. H., Olayinka, O. O., and Tope-Ajayi, O. O.(2016).Mapping of Traffic-Related Air *Pollution* Using GIS Techniques in Ijebu-Ode, Nigeria. The Indonesian Journal of Geography, 48 (1) (2016), 76-86.

Aganaba-Jeanty T., and Huggins, A. (2019). Satellite measurement of GHG emissions: Prospects for enhancing transparency and answerability under international law. *Transnational Environmental Law* , *8*(2), 303-326.

Agbozu, I. E., and Oghama, O. E. (2022).Spatial and diurnal distribution of carbon monoxide (CO) and its health and environmental implications in selected locations in the Niger Delta Area of Nigeria.*African Journal of Science, Technology, Innovation and Development*, *14*(5), 1327-1336.

Al-Mahdi, A. M., and Maina, M. L. (2013). The role of GIS and remote sensing in mapping the *distribution* of greenhouse gases. *European Scientific Journal* , *9*(36), 404-410. DOI: 10.19044/ESJ.2013.V9N36P

Anand, J. S., and Monks, P. S. (2017). Estimating daily surface NO2 concentrations from satellite data–a case study over Hong Kong using land use regression models. *Atmospheric Chemistry and Physics*, *17*(13), 8211-8230.

Bugdayci, I., Ugurlu, O., and Kunt, F. (2023).Spatial Analysis of SO_2, PM10, CO, NO_2, and O_3 Pollutants: The Case of Konya Province, Turkey.*Atmosphere*, *14*(3), (2023), 462.

Busa, E., Gugamsetty, B., Kalluri, R. O. R., Kotalo, R. G., Tandule, C. R., Thotli, L. R.,Chakala, M. and Palle, S. N. R. (2022). Diurnal, seasonal, and vertical distribution of carbon monoxide levels and their potential sources over a semi-arid region, India, Atmósfera, *35*(1),165-178.

Chukwuma E., Nwajinka, C., Orakwe, L. and Odoh, C.(2018). GIS-Based Estimate of GHG *Emission* from Livestock in Anambra State of Nigeria.*Biotechnology Journal International*,*21*(2): 1-8.

David-Okoro, I. L., Chineke, T. C., Nwofor, O. K., Opara, A. I., Ewurum, N. B. B., Nwosu, E. and Chinaka, J. C. (2023). Sampling Five Criteria Air Pollutant over Nigeria from 2005 to 2018 using NASA GIOVANNI Air Quality. International Journal of Innovative Science and Research Technology, 8 (5), 3703 – 3712.

Dehkordi, M. H. R., Isfahani, A. H. M., Rasti, E., Nosouhi, R., Akbari M., and Jahangiri, M. (2022). Energy-Economic-Environmental assessment of solar-wind-biomass systems for finding the best areas in Iran: A case study using GIS maps.*Sustainable Energy Technologies and Assessments*, *53*, 102652.

Delta State Ministry of Economic Planning (2022).Delta State Medium Term Development Plan II (2020-2023). Asaba, Delta State Ministry of Economic Planning, (2022).

Egbe, O. E (2013).Modelling Land Cover Change in Edo and Delta States, Nigeria. Ann Arbor, ProQuest LLC(2013).

Egwunatum, A. E., Ndulue, N. B. and Okoro, V. I. (2022). Assessment of fuelwoodutilization and carbon emission on conservation of Mangrove (*Rhizophora racemosa*) forest in Koko, Delta state, Nigeria. International Journal of Forestry, Ecology and Environment, 06(01), 215-223. https://doi.org/10.18801/ijfee.060122.24

Erawan, M., Karuniasa, M., and Kusnoputranto, H. (2021). Line source dispersion and spatial distribution of carbon monoxide concentration on Daan Mogot Street, Tangerang City, Jabodetabek Metropolitan Area.Earth and Environmental Science, 716:(2021). doi:10.1088/1755-1315/716/1/012025

European Space Agency (2020).Satellites providing clear picture of greenhouse gases. Available at: https://www.esa.int/Applications/Observing_the_Earth/Space_for_our_climate/ Satellites_providing_clear_picture_of_greenhouse_gases (accessed 24 March, 2023)

Filonchyk, M., Hurynovich, V., Yan, H., Gusev, A., and Shpilevskaya, N.(2020). Impact assessment of COVID-19 on variations of SO_2, NO_2, CO and AOD over East China.*Aerosol and air quality research*, *20*(7), (2020), 1530-1540.

Forster, P. M., Smith, C. J., Walsh, T., Lamb, W. F., Lamboll, R., Hauser, M, A., Ribes, D., *Rosen*, N., Gillett, M. D., and Zhai, P. (2023). Indicators of Global Climate Change 2022: annual update of large-scale indicators of the state of the climate system and human influence. Earth *System Science Data*, *15*(6), 2295-2327.

Garajeh, M. K., Salmani, B., Naghadehi, S. Z., Goodarzi, H. V., and Khasraei A (2023). An integrated approach of remote sensing and geospatial analysis for modeling and predicting the impacts of climate change on food security.*Scientific Reports*, *13*(1), 1057. https://doi.org/10.1038/s41598-023-28244-5

Granier, C., Darras, S. H., Denier van der Gon, J., Doubalova, N., Elguindi, B., Galle, M., Gauss, M., Guevara. J.-P., Jalkanen, J., Kuenen, C., Liousse, B., Quack, D., Sindelarova, S. K.(2019). The Copernicus Atmosphere Monitoring Service global and regional emissions (April 2019 version). Copernicus Atmosphere Monitoring Service (CAMS) report (2019). Doi:10.24380/d0bn-kx16.

Hashim, M., Ng, H. L., Zakari, D. M., Sani, D. A., Chindo, M. M., Hassan N. and Pour, A. B, (2023). Mapping of greenhouse gas concentration in Peninsular Malaysia Industrial Areas using unmanned aerial vehicle-based sniffer sensor.*Remote Sensing*, *15*(1), 255.

Hink, J. K., Wogalter, M. S., and Eustace, J. K. (1996). Display of quantitative information: are grables better than plain graphs or tablesş". In *Proceedings of the Human Factors and* Ergonomics *Society Annual Meeting* 40(23), 1155-1159. Sage CA: Los Angeles, CA: SAGE Publications.

Höglund-Isaksson L. (2012). Global anthropogenic methane emissions 2005–2030: technical mitigation potentials and costs. Atmospheric Chemistry & Physics 12 (2012), 9079-9096.

Hui, D., Deng, Q., Tian, H., and Luo Y (2022). Global climate change and greenhouse gases emissions in terrestrial ecosystems. In *Handbook of climate change mitigation and adaptation*. Cham: Springer, (2022), 23-76.

Ibanga, O. A.. Idehen O. F and Omonigho M. G (2022). Spatiotemporal Variability of Soil Moisture under Different Soil Groups in Etsako West Local Government Area, Edo State, Nigeria. Journal of the Saudi Society of Agricultural Science, 22 (2), (2022), 125-147. doi: https://doi.org/10.1016/j.jssas.2021.07.006

Junker C. and Liousse, C. (2008). A global emission inventory of carbonaceous aerosol from historic records of fossil fuel and biofuel consumption for the period 1860-1997. Atmospheric Chemistry & Physics 8, 1195–1207.

Klimont, Z., Smith, S. J. and Cofala, J. (2013). The last decade of global anthropogenic sulfur dioxide: 2000–2011 emissions. EnvironmentalResearch Letters 8 (2013), 014003.

Mamatkulova, S., Uzakov, G., Abduvaliyev, A., Tuxliyev, I., and Saidov, J. (2022).Improvement of *the* GIS map of the potential of biomass for the development of bioenergy production in the Republic of Uzbekistan", *AIP Conference Proceedings,* 2432 (1),2432, 060010 *https://doi.org/10.1063/5.0089601*

Manabe,S. (2019). Role of greenhouse gas in climate change.*Tellus A: Dynamic Meteorology and Oceanography* 71(1): 1620078.

Mejía, D., Alvarez, H., Zalakeviciute, R., Macancela, D., Sanchez, C. and Bonilla, S. (2023). Sentinel satellite data monitoring of air pollutants with interpolation methods in Guayaquil, Ecuador. *Remote Sensing Applications: Society and Environment*, *31*, (2023), 100990.

Mikhaylov, A., Moiseev, N., Aleshin, K., and Burkhardt, T. (2020). Global climate change and greenhouse effect. Entrepreneurship *and Sustainability Issues7*(4), 2897.

Mobolade D. T. and Pourvahidi P. (2020). Bioclimatic approach for climate classification of Nigeria.*Sustainability*, *12*(10), 4192.

National Population Commission (NPC) (2010). 2006 Population and housing census: population distribution by Sex, State, LGA and Senatorial District. Priority Table, 3. Abuja, NPC (2010).

Neale, R. E., Barnes, P. W., Robson, T. M., Neale, P. J., Williamson, C. E., Zepp, R. G., Zepp, S. R. S., Wilson, A. L., Andrady, M., and Zhu, M. (2021). Environmental effects of stratospheric ozone depletion, UV radiation, and interactions with climate change: UNEP Environmental Effects Assessment Panel, Update 2020.*Photochemical & Photobiological Sciences*, *20* (1), 1-67.

Nguyen, A. T., Némery, J. Gratiot, N. Dao, T. S. Le, T. T. M. Baduel C. and Garnier J., (2022). Does eutrophication enhance greenhouse gas emissions in urbanized tropical estuariesş.*Environmental Pollution*, *303*, 119105.

Obiefuna, J. N., Inah, E. O., Atsa, J. W. U., and Etim, E. A. (2021). Geospatial Assessment of Ambient Air Quality Footprints in Relation to Urban Landuses in

Nigeria.*Environment and Ecology Research*, *9*, (2021), 426-446.
Okoh, R. H. (2013).Biophysical and Socio-Economic Assessment of the Nexus of Environmental Degradation and Climate Change, Delta State, Nigeria". Assessment Report submitted to Territorial Approach to Climate Change (TACC) in Delta State, Climate Change Unit, Ministry of Environment, Delta State, Nigeria, (2013), 22.
Okpobiri, O., Rowand, E. D., Egobueze, F. E. and Chinwe, M. F. (2023).Monitoring and *Quantification* of Carbon Dioxide Emissions and Impact of Sea-Surface Temperature on Marine Ecosystems as Climate Change Indicators in the Niger Delta Using Geospatial Technology. Journal of Atmospheric Science Research. 6(1), (2023), 1-20. DOI: https://doi.org/10.30564/jasr.v6i1.5107
Opio, R., Mugume, I. and Nakatumba-Nabende, J. (2021). Understanding the Trend of NO_2, $SO_2$and CO over East Africa from 2005 to 2020. *Atmosphere*, *12*(10), (2021), 1283.
Peel, M. C., Finlayson, B. L., and McMahon, T. A. (2007). Updated world map of the Köppen-Geiger Climate classification. *Hydrol. Earth Syst. Sci. 11*, 1633-1644.
Salami, V. T., Ahmad, S. H., James, G. K. Jega, I. M., Adedeji, O. I., Ajayi, O. O. and Sanusi U. (2019). Geospatial Evaluation of Carbon Dioxide Pollutant Concentration in Federal Capital Territory, Nigeria.*International Journal of Innovative Science and Research Technology*, *4*(2), (2019), 527-535.
Salonen, H. Salthammer T. and Morawska, L. (2019). Human exposure to NO_2 in school and office indoor environments.*Environment International*, *130*, (2019), 104887.
Savenets, M., Dvoretska, I., Nadtochii, L. and Zhemera N. (2022). Comparison of TROPOMI NO_2, CO, HCHO, and SO_2 data against ground-level measurements in close proximity to large anthropogenic emission sources in the example of Ukraine.*Meteorological Applications*, *29*(6), (2022). e2108.
Science Learning Hub (2018). Pokapū Akoranga Pūtaiao, Measuring greenhouse gasemissions.*Available* at: https://www.sciencelearn.org.nz/resources/2630-measuring-greenhouse- gas-emissions (accessed 24 March, 2023)
Sheel, V., Sahu, L. K., Kajino, M., Deushi, M., Stein, O. and Nedelec, P. (2014). Seasonal and interannual variability of carbon monoxide based on MOZAIC observations, MACC reanalysis, and model simulations over an urban site in India.*Journal of Geophysical Research: Atmospheres*, *119*(14), (2014), 9123-9141.
Shehu, M. S., Umaru, I. Adedeji, O. Mundi, A. A. and Lawal, R. S. (2019). Theoretical Confirmation of Seasonal and Solar Radiation Impacts on Outdoor Atmospheric Aerosols (PM2. 5, SO_2 and CO) in FCT Abuja, Nigeria. International Journal of Innovation and Scientific Research 44(2), (2019), 186–194.
Sîrbu O. M., Vîlceanu, C. B., Moscovici, A. M., and Herban, S.(2022). Open-Source GIS for *Territorial* Planning-Solar Map of Timiș County, Romania.*Scientific Papers. Series E. Land Reclamation, Earth Observation & Surveying, Environmental Engineering*, *11 444*-451.
Thorpe, A. K., Dennison, P. E., Guanter, L. Frankenberg C. and Aben, I. (2022). Special issue on remote sensing of greenhouse gas emissions.*Remote Sensing of Environment*, *277,*113069. DOI: 10.1016/j.rse.2022.113069
Ugboma P. P. (2023). Effects of Deforestation on Soil Fertility in Delta State, Nigeria. Published PhD Thesis, Delta State University, Abraka. Available at: https://www.delsu.edu.ng/clt/ Effects%20OF%20DEFORESTATION%20ON%20SOIL%20FERTILITY%20IN%20DELTA%20STATE,%20NIGERIA.pdf. (accessed 22 June 2023)
World Health Organization, (2021).WHO global air quality guidelines: particulate matter (PM2.5 and PM10), ozone, nitrogen dioxide, sulfur dioxide and carbon monoxide. World Health Organization, (2021). Available at: https://apps.who.int/iris/handle/10665/345329. (accessed 22 June 2023).
Xi-Liu, Y. U. E., and Qing-Xian, G. A. O. (2018). Contributions of natural systems and human *activity* to greenhouse gas emissions.*Advances in Climate Change Research*, *9* (4):243-252.

Acknowledgement

This study was funded by the Energy Commission of Nigeria, Abuja. The authors will like to appreciate the Director General/Chief Executive Officer of the Commission, Abuja and the Director, National Centre for Energy and Environment, University of Benin for approving and funding this Project.